JOURNAL OF NANO- AND ELECTRONIC PHYSICS
Vol. **18** No 3, 03029(7pp) (2026)

ЖУРНАЛ НАНО- ТА ЕЛЕКТРОННОЇ ФІЗИКИ
Том **18** № 3, 03029(7cc) (2026)

OPEN ACCESS

REGULAR ARTICLE

Electronic Energy Structure of Sc-doped GaAs

H.A. Ilchuk[1], I.V. Semkiv[1], S.I. Krukovskyi[1,2], O.S. Kushnir[3], B. Andriyevsky[4], A.I. Kashuba[1,*]

[1] *Lviv Polytechnic National University, 79013 Lviv, Ukraine*
[2] *Scientific Research Company 'Electron-Carat', 79031 Lviv, Ukraine*
[3] *Ivan Franko National University of Lviv, 79017 Lviv, Ukraine*
[4] *Koszalin University of Technology, 75453 Koszalin, Poland*

(Received 20 February 2026; revised manuscript received 18 June 2026; published online 26 June 2026)

Gallium arsenide (GaAs) exhibits a wide range of practical applications. Notably, it is extensively employed in optoelectronics, where it serves as a foundation for high-efficiency light-emitting diodes, laser diodes, photodetectors, and photovoltaic cells. Additional significant applications include radiation-resistant solar arrays, integrated circuits, and Hall-effect sensors, among others. In this study, we report the concentration dependence of the electronic energy structure for Sc-doped GaAs ($Ga_{1-x}Sc_xAs$, x = 1/32, 2/32 and 8/32). The calculations were performed within the Density Functional Theory (DFT) framework using the Generalized Gradient Approximation (GGA) with the Perdew–Burke–Ernzerhof (PBEsol) parametrization. The interaction between ions and valence electrons was described using norm-conserving pseudopotentials. Two alternative cases of Sc doping in GaAs ($Ga_{1-x}Sc_xAs$, x = 2/32) are investigated, which correspond to either cubic (the space group #215) or tetragonal (#115) structures. The energy band dispersion and the density of states are analyzed. It was found that the band gap is characterized by a direct transition at low ($x \leq 2/32$) Sc concentrations, whereas it shifts to an indirect type at high (x = 8/32) Sc doping levels. The energy band dispersion was analyzed based on the calculated effective masses of electrons (m_c) and holes (m_v). The effect of scandium doping on the electronic energy structure of GaAs was elucidated based on the partial density of states (PDOS) contributions. Issuing from the electronic energy spectrum, we calculate the real and imaginary components of the dielectric function. Finally, the fundamental optical properties of the $Ga_{1-x}Sc_xAs$ solid solutions are derived using the Kramers–Kronig relations, in particular the refractive index and the extinction and absorption coefficients.

Keywords: GaAs, Electronic energy structure, Density of states, Bandgap, Refractive index, Optical dielectric function.

DOI: 10.21272/jnep.18(3).03029 PACS numbers: 71.15.Mb, 71.20. – b

1. INTRODUCTION

Gallium arsenide (GaAs) is a versatile semiconductor material widely utilized in numerous highly technological fields. In the domain of optoelectronics, it serves as a fundamental material for high-performance light-emitting diodes (LEDs) [1, 2], laser diodes [3], photo-detectors, photovoltaic cells [4], etc. Furthermore, its exceptional electronic properties make it critical for different radio-frequency (RF) applications, specifically in the radar and satellite-based communications [5]. The applicability of GaAs also encompasses radiation-resistant solar arrays [6], high-speed integrated circuits [7], and the sensors based upon Hall effect [8].

Gallium arsenide is characterized by a cubic crystal structure of a zinc-blende type. It belongs to the space symmetry group F-43m, while the appropriate lattice parameter reported in Ref. [9] is equal to a = 5.6537 Å. GaAs reveals a direct bandgap, which is characterized by the energy width close to 1.42 eV at the room temperature [10].

The fundamental electronic and optical parameters of GaAs-based materials can be modulated for different purposes through their doping and so formation of solid solutions. For example, a low-level (< 0.05 at. %) doping of GaAs with rare-earth elements (e.g., Yb, Ce or Ho) induces an n-to-p conduction inversion [11]. To be specific, Ce-doped GaAs exhibits a p-type conductivity when the dopant concentration exceeds ~ 0.043 at. % [11]. As a consequence, doping of GaAs with the rare-earth elements can streamline the development of novel $p^+/i/n^+$ structures, with the unique features of their electronic spectrum. Therefore any investigations of the rare-earth doped GaAs solid solutions seem to be of primary importance, at least from the practical viewpoint.

In this respect it would be natural to study theoretically the electronic spectra of the solid solutions mentioned above, prior to any practical attempts at the synthesis of those materials. In this respect, density functional theory abbreviated as DFT represents a cornerstone computational framework for analyzing the electronic structure [12, 13]. Note that, in contrast to the extensively documented properties of GaAs itself [14], the theoretical calculation data concerned with the electronic energy spectrum of Sc-doped GaAs remains limited. Although Sc-doped GaAs has been already explored by the

* Correspondence e-mail: andrii.i.kashuba@lpnu.ua

© 2026 The Author(s). Journal of Nano- and Electronic Physics published by Sumy State University. This article is distributed under the terms and conditions of the Creative Commons Attribution (CC BY) license.

Cite this article as: H.A. Ilchuk et al., *J. Nano- Electron. Phys.* 18 No 3, 03029 (2026) https://doi.org/10.21272/jnep.18(3).03029

authors [15], their study has its focus exclusively on a single Sc concentration, $x = 1/32$. This has been done with the aid of local density approximation (LDA) for the exchange-correlation potential and ultrasoft pseudo-potentials for description of ion-valence interactions [15].

In the present work, we study the electronic energy structure of Sc-doped GaAs, i.e. the solid solutions $Ga_{1-x}Sc_xAs$ ($x = 1/32$, 2/32 and 8/32). The calculations are carried out within the DFT framework and employ a generalized gradient approximation along with a known Perdew–Burke–Ernzerhof parametrization for solids [16]. The ion-valence interactions are described using norm-conserving pseudo-potentials [17]. A characteristic feature of the present work is investigation of a structural change from cubic to tetragonal crystalline structure, which occurs in a doped compound $Ga_{30}Sc_2As_{32}$. Another peculiarity of our study is application of the computational techniques mentioned above in the particular context of Sc-doped GaAs. As a result, we have analyzed the optical properties of Sc-doped GaAs from the electronic energy spectrum calculated. Specifically, the spectral dependences of the absorption coefficient and the refractive index of $Ga_{1-x}Sc_xAs$ have been found.

2. METHODS OF CALCULATIONS

As stated above, our DFT-based calculations encompassed geometry optimization and further analysis of the total energy, the electronic spectra, the density of states (DOS), and the optical properties. They were done in the generalized gradient approximation and employed the Perdew–Burke–Ernzerhof parametrization for solids [16]. In order to describe accurately the interactions between ions and valence electrons, we integrated the exchange-correlation functional with the norm-conserving pseudo-potentials [17]. The details for the theoretical parameters used in our calculations are presented in Table 1.

We modeled Sc-doped GaAs with the concentrations $x = 1/32$, 2/32 and 8/32 in the following manner. First, a $2 \times 2 \times 2$ super-cell of the initial compound GaAs was formed. The next stage was theoretical construction of solid-state $Ga_{1-x}Sc_xAs$ solutions. Ga atoms were gradually replaced by Sc in the optimized GaAs structure. To model this substitution, the optimized crystalline structure of GaAs was changed to triclinic, with the space symmetry $P1$. Finally, the crystalline structures of $Ga_{1-x}Sc_xAs$ were optimized and their parameters were found. Note that the compound $Ga_{30}Sc_2As_{32}$ with the concentration $x = 2/32$ was optimized for the both cases of tetragonal (the space group #115) and cubic (the space group #215) structures.

Table 1 – Parameters used in our calculations

$E_{cut\text{-}off}$, eV	Total energy convergence threshold, eV/atom	k-point grid [18]	Residual forces on atoms, eV/Å	Maximum atomic displacements, Å	Internal stresses, GPa
880	$5 \cdot 10^{-6}$	$2 \times 2 \times 2$	0.01	$5.0 \cdot 10^{-4}$	0.02

3. RESULTS AND DISCUSSION

A single location position of the Sc atoms in the parent structure of GaAs has been considered for the $Ga_{1-x}Sc_xAs$ solid solutions ($x = 1/32$, 2/32 and 8/32). It is worthwhile that the substitution of Ga with Sc atoms imposes a structural change from the spatial symmetry group $F\text{-}43m$ (for GaAs) to $P\text{-}43m$ (for $Ga_{1-x}Sc_xAs$ with $x = 1/32$, 2/32 and 8/32) or $P\text{-}4M2$ (for $Ga_{1-x}Sc_xAs$ with $x = 2/32$). The space groups of symmetry and the lattice parameters found for the optimized structures of $Ga_{1-x}Sc_xAs$ are also summarized in Table 2. Additionally, Table 2 presents the total energy values for the optimized configurations obtained by us. Finally, it can be seen from Table 2 that the increase in the number of Sc atoms in the GaAs super-cell, i.e. the increase in the Sc concentration x, leads to decreasing material density.

The electronic energy band diagrams for Sc-doped GaAs calculated along the high-symmetry points of the Brillouin zone are displayed in Fig. 1. Since the electronic band structure and the optical parameters of the parent GaAs compound has already been detailed in the literature (see Ref. [19]), they are omitted from the present work. In all of the plots in Fig. 1, the energy scale is referenced to the Fermi level $E_F = 0$ eV.

The analysis of our calculated energy spectra reveals that, in case of the concentrations $x = 0$, 1/32 and 2/32, the minimum optical bandgap remains localized at the center of the Brillouin zone (the Γ-point). Consequently, the crystal maintains a direct energy bandgap at these concentrations. Note that both the cubic and tetragonal phases of the Sc-doped compound with $x = 2/32$ exhibit the direct bandgap. The primary distinction of these phases lies in the bandgap values, which are equal respectively to $E_g^{cub} = 1.026$ eV and $E_g^{tet} = 0.930$ eV. A similar effect of reduction in the bandgap for the tetragonal structure of La-doped GaAs has been reported in Ref. [19]. Finally, our total-energy calculations have shown that formation of the tetragonal structure is energetically less favorable, if compared with the cubic structure (see the data in Table 2).

The minimum energy gap observed at the scandium doping level $x = 8/32 = 0.25$ becomes of an indirect type. It is noteworthy, however, that the energy difference between the indirect transition and the corresponding direct transition at the Γ-point is less than 0.023 eV (see Table 3).

Table 2 – Some structural parameters of Sc-doped GaAs: 'S. G.' implies 'space group'

x	S. G.	S. G. #	a, Å	c, Å	V, Å^3	E_{total}, eV	ρ, g·cm^{-3}	Supercell
0	$F\text{-}43m$	216	5.650075	–	180.37	– 7522.76	5.33	$1 \times 1 \times 1$
1/32	$P\text{-}43m$	215	11.328577	–	1453.87	– 58523.86	5.26	$2 \times 2 \times 2$
2/32	$P\text{-}43m$	215	11.389425	–	1477.42	– 56865.68	5.19	$2 \times 2 \times 2$
2/32	$P\text{-}4M2$	115	8.041805	11.495273	1497.58	– 26774.98	5.06	$2 \times 2 \times 1$
8/32	$P\text{-}43m$	215	5.764538	–	191.56	– 5864.26	4.80	$1 \times 1 \times 1$

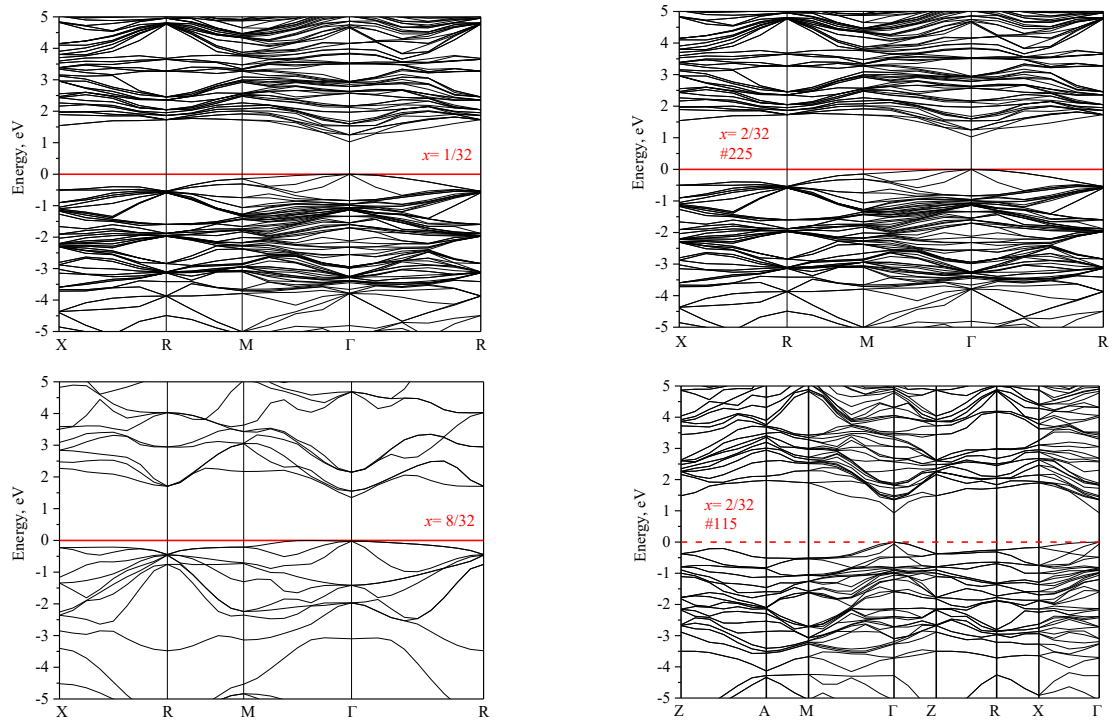

Fig. 1 – Electronic band energy structures of $Ga_{1-x}Sc_xAs$ solid solutions (see the legend). Red lines correspond to the positions of the Fermi level

These results suggest that doping of cubic GaAs with Sc at the concentration $x = 0.25$ induces a direct-to-indirect bandgap transition. Consequently, we suggest that Sc-doped GaAs can indeed facilitate a development of $p^+/i/n^+$ structures, whenever one provides a gradient distribution of Sc impurity concentration across different layers of the structure.

Considering the values of the minimum bandgap for each of the concentrations under test, one can see that the bandgap width increases with increasing Sc concentration in $Ga_{1-x}Sc_xAs$. In addition, the data shown in Fig. 1 confirm a clear anisotropy difference $E(\mathbf{k})$ between the valence and conduction bands. The complex valence top is flatter, which is naturally explained by the fact that holes are less mobile than electrons ($\mu \sim 1/m^*$). This behavior is caused by the inverse relationship between the effective mass of electron (m_c) or hole (m_v) and the spread $E(\mathbf{k})$ of energy levels [20, 21]:

$$\frac{1}{m^*} = \frac{4\pi^2}{h^2}\frac{\mathrm{d}^2 E(k)}{\mathrm{d}k^2}. \qquad (3.1)$$

In Eq. (1), h denotes the Planck constant and $E(\mathbf{k})$ implies the dependence of the band energy E on the electron wave vector $\mathbf{k}$. Table 3 presents the effective mass values obtained for Sc-doped GaAs from the electronic energy band diagrams along different directions in the $\mathbf{k}$-space.

The effective masses of electron ($m_c^{\text{M-Γ-R}} = 0.070m_e$, with m_e denoting the free electron mass) and hole ($m_v^{\text{M-Γ-R}} = 0.940m_e$) found by us agree well with the known literature data [26]. The dependence of the effective electron mass m_c on the Sc concentration in $Ga_{1-x}Sc_xAs$ exhibits a sharp increase near the concentration point $x = 1/32$ and then decreases gradually. A qualitatively similar dependence on the Sc concentration in $Ga_{1-x}Sc_xAs$ is observed for the effective mass of hole m_v.

We have determined the total and partial electronic DOS for Sc-doped GaAs from the energy structures calculated as above (see Fig. 2). The energy levels near – 15 eV are attributed to the d-states of Ga and As atoms, while the s-states of Ga predominate around – 10 eV. The region between – 7 and – 5 eV can be primarily attributed to the s-states of Ga. The valence-band maximum is formed by the p-states of As with an admixture of the p-states of Ga, whereas the conduction-band minimum consists of the s- and p-states of both Ga and As. In accordance with the Pauli Exclusion Principle, the minimum energy gap arises from the s–p transitions associated with Ga–As bonding. Upon Sc doping, the s- and d-states of Sc contribute more and more to the valence-band maximum, while the p- and d-states of Sc participate in formation of the conduction-band minimum (see Fig. 2). Finally, we suggest that the direct-to-indirect bandgap transition observed at $x \approx 0.25$ can be attributed to the influence of the d-states of Sc (see Fig. 1).

Based on the calculated electronic energy structures for Sc-doped GaAs, we have determined the spectral dependences of the real (ε_1) and imaginary (ε_2) parts of the complex dielectric function $\varepsilon(h\nu) = \varepsilon_1 + i\varepsilon_2$:

$$\varepsilon_1 - 1 = \frac{2}{\pi}\int_0^\infty \frac{t\varepsilon_2(t)dt}{t^2 - (\hbar\omega)^2}, \qquad (3.2)$$

$$\varepsilon_2 = \frac{2e^2\pi}{V\varepsilon_0}\sum_{K,v,c}\left|\left\langle\psi_K^c\left|\hat{u}\cdot r\right|\psi_K^v\right\rangle\right|^2 \delta\left(E_K^c - E_K^v - \hbar\omega\right). \qquad (3.3)$$

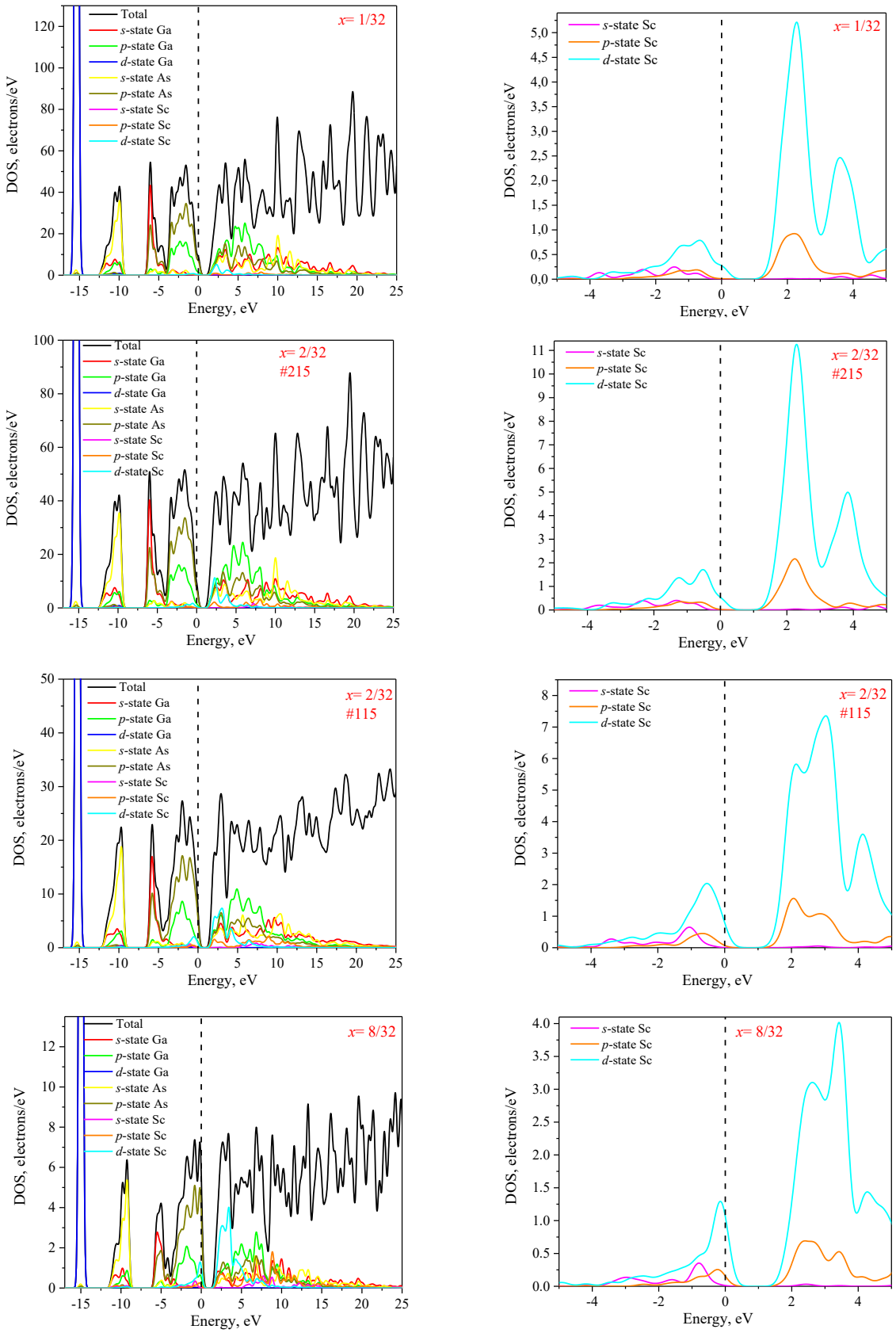

Fig. 2 – DOS calculated for $Ga_{1-x}Sc_xAs$ with different Sc concentrations. Right panels in the figure correspond to partial distributions of electronic DOS for Sc

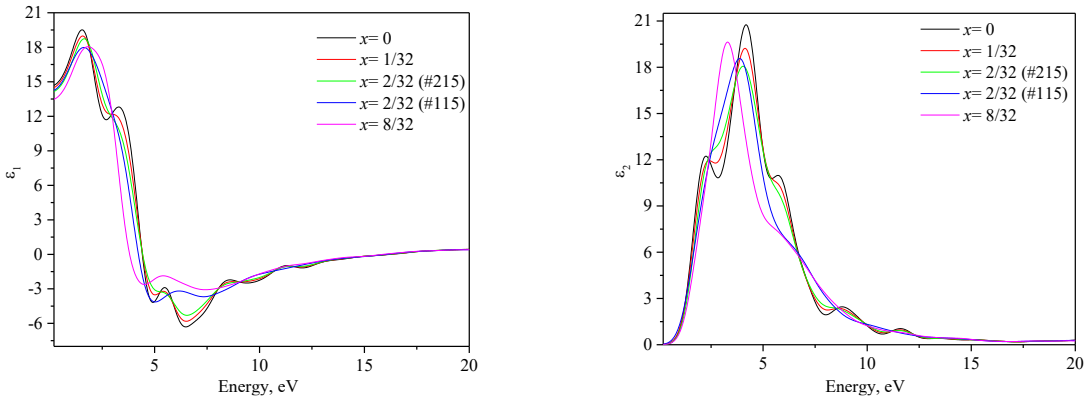

Fig. 3 – Real (ε_1) and imaginary (ε_2) parts of the dielectric permittivity ε calculated for $Ga_{1-x}Sc_xAs$ with different Sc concentrations (see the legends)

Table 3 – Energy-related properties of Sc-doped GaAs. The indices '*c*' and '*v*' refer to the conduction and valence bands, respectively

X	S. G. #	E_g^{dir}, eV	E_g^{indir}, eV	ΔE, eV	$m_c^{M\text{-}\Gamma\text{-}R}/m_e$	$m_v^{M\text{-}\Gamma\text{-}R}/m_e$
0	216	0.823	–	–	0.070	0.940
1/32	215	0.893	–	–	0.570	2.816
2/32	215	1.026	–	–	0.570	2.816
2/32	115	0.930	–	–	0.138	0.302
8/32	215	1.372	1.349	0.023	0.145	1.987

The spectral dependences of the real and imaginary parts of the dielectric permittivity are shown in Fig. 3. The dependence of the real part ε_1 exhibits peaks in the vicinities of 1.5 and 3.3 eV. The peak located at approximately 1.5 eV undergoes a blue shift with increasing x value. The behavior of this peak is analogous to the concentration dependence of the bandgap (see Table 3). The peak nearby 3.3 eV is quenched with increasing Sc concentration in $Ga_{1-x}Sc_xAs$. It is no longer observed at the concentrations higher than $x = 2/32$. The imaginary part ε_2 of the dielectric permittivity exhibits a somewhat more complex spectral behavior. For the pure GaAs compound, three peaks are observed near 2.2, 4.2 and 5.8 eV. The main peak located at approximately 4.2 eV for the concentration $x = 0$ undergoes a red shift as the Sc concentration increases.

Based on the spectral dependences of the ε_1 and ε_2 parameters, one can determine the dispersion of the refractive index n and the extinction coefficient k:

$$n = \sqrt{\frac{(\varepsilon_1^2 + \varepsilon_2^2)^{1/2} + \varepsilon_1}{2}}, \qquad (3.4)$$

$$k = \sqrt{\frac{(\varepsilon_1^2 + \varepsilon_2^2)^{1/2} - \varepsilon_1}{2}}. \qquad (3.5)$$

These results are presented in Fig. 4. Here the spectral dependences of the refractive index and the extinction coefficient are similar respectively to those of the real and imaginary parts of the dielectric permittivity. Finally, we have evaluated the spectral dependence of the absorption coefficient α, using the relation

$$\alpha = \frac{4\pi k}{\lambda}. \qquad (3.6)$$

The spectral dependence of α is given by Fig. 5. Note that the absolute values of the absorption coefficient calculated by us conform well to the data reported in Ref. [22].

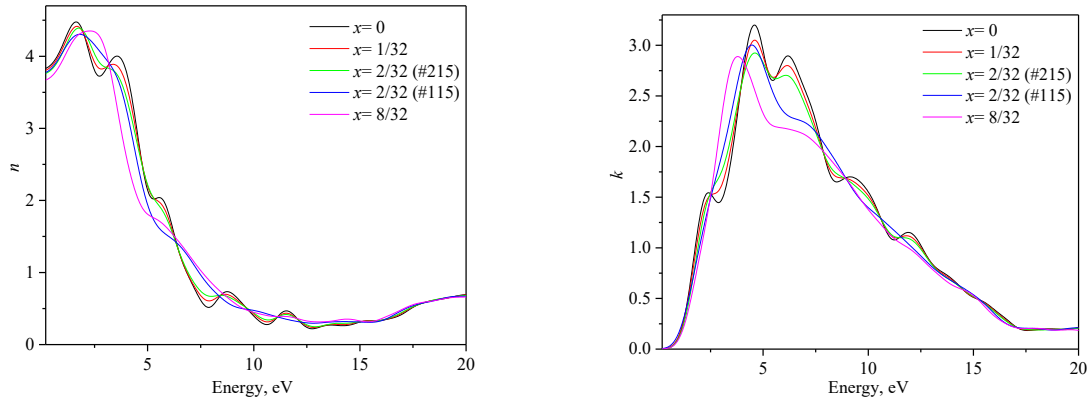

Fig. 4 – Refractive index n and extinction coefficient k calculated for Sc-doped GaAs

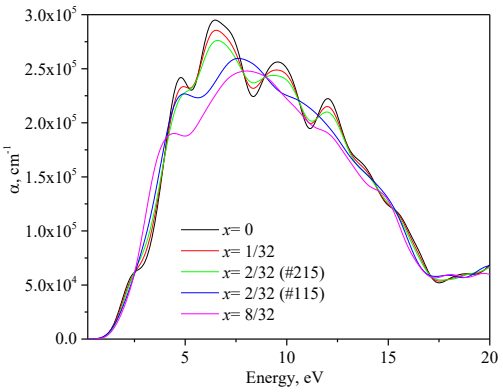

Fig. 5 – Absorption coefficient α calculated for Sc-doped GaAs

4. CONCLUSION

The electronic energy structure of Sc-doped GaAs has been calculated for the Sc concentrations $x = 1/32$, 2/32 and 8/32 in the framework of the DFT. We have shown that the material density decreases with increasing Sc concentration in $Ga_{1-x}Sc_xAs$. The analysis of the electronic energy structure of these solid solutions reveals that the compound with the Sc concentration $x = 8/32$ is characterized by the indirect optical transitions (E_g^{indir}), whereas the compounds $Ga_{1-x}La_xAs$ with $x = 1/32$ and 2/32 exhibit the direct bandgap transitions (E_g^{dir}). The concentration dependence of the bandgap width shows a decreasing behavior with increasing Sc concentration. Both the cubic and tetragonal phases of Sc-doped GaAs obtained at $x = 2/32$ are characterized by the direct bandgap. The primary quantitative distinction of these phases is their bandgap values. Based on the total energy calculations, the tetragonal structure is found to be energetically less favorable than the cubic structure.

We have also analyzed the energy band dispersion and have calculated the effective masses of electrons and holes for Sc-doped GaAs. Following from the electronic energy spectra, we have ascertained the total and partial DOS of these solid solutions. The *d*-states of Sc are found to influence formation of the minimum of the conduction band and the maximum of the valence band. Finally, the spectral dependences of the primary optical functions have been calculated for $Ga_{1-x}La_xAs$. These are the real and imaginary parts of the complex dielectric permittivity ε, the refractive index n, the extinction coefficient k, and the absorption coefficient α.

FUNDING AND ACKNOWLEDGEMENTS

This work was supported by the National Research Foundation of Ukraine under the Project No. 2025.07/0258 "Development of novel *p*+/*i*/*n*+ structures based on gallium arsenide thin films". A part of our computer calculations were performed at the Interdisciplinary Center for Mathematical and Computational Modeling of Warsaw University, Poland (the Project No. g 104-2591) and the Wrocławskie Centrum Sieciowo-Superkomputerowe of the Wrocław University of Technology, Poland (the Project No. 053).

REFERENCES

1. T. Takagi, H. Imamoto, F. Sato, K. Imanaka, M. Shimura, *IEEE Photon. Technol. Lett.* **1**, 14 (1989) https://doi.org/10.1109/68.87880.
2. M. Premkumar, M. Arun, S. Sathiya Priya, D. Kalaiarasi, R. Prathipa, *Mater. Today: Proc.* **80**, 1932 (2023) https://doi.org/10.1016/j.matpr.2021.05.650.
3. S.S. Ou, J.J. Yang, M. Jansen, *Appl. Phys. Lett.* **57**, 1861 (1990) https://doi.org/10.1063/1.104039.
4. X. Dai, S. Zhang, Z. Wang, G. Adamo, G.G. Liu, Y. Huang, C. Couteau, C. Soci, *Nano Lett.* **14**, 2688 (2014) https://doi.org/10.1021/nl5006004.
5. K.J. Schopf, E. Pettenpaul, *3rd International Workshop on Integrated Nonlinear Microwave and Millimeterwave Circuits*, 59 (1994) https://doi.org/10.1109/INMMC.1994.512513.
6. M. Yamaguchi, *Sol. Energy Mater. Sol. C.* **68**, 31 (2001) https://doi.org/10.1016/S0927-0248(00)00344-5.
7. M. Shur, *GaAs Digital Integrated Circuits* (Boston: Springer: 1987) https://doi.org/10.1007/978-1-4899-1989-2_9.
8. R. Campesato, C. Flores, A. Passaseo, S. Verni, *Sensor. Actuat. A: Phys.* **32**, 651 (1992) https://doi.org/10.1016/0924-4247(92)80058-B.
9. R.W.G. Wyckoff, *ZnS Structure, Sphalerite Structure. Crystal Structures*. (New York: Interscience Publishers: 1963).
10. M. El Allali, C.B. Sørensen, E. Veje, P. Tidemand-Petersson, *Phys. Rev. B* **48**, 4398 (1993) https://doi.org/10.1103/PhysRevB.48.4398.
11. S. Krukovskyi, R. Krukovskyi, H. Ilchuk, E. Zmiiovska, I. Semkiv, *14th International Conference on Advanced Trends in Radioelectronics, Telecommunications and Computer Engineering (TCSET-2018) Proceedings*, 462 (2018) https://doi.org/10.1109/TCSET.2018.8336241.
12. H. Ilchuk, E. Zmiiovska, R. Petrus, I. Semkiv, I. Lopatynskyi, A. Kashuba, *J. Nano- Electron. Phys.* **12**, 01027 (2020) https://doi.org/10.21272/jnep.12(1).01027.
13. M.Ya. Rudysh, *Mater. Sci. Semicond. Proc.* **148**, 106814 (2022) https://doi.org/10.1016/j.mssp.2022.106814.
14. A. Baldereschi, K. Maschke, E. Hess, H. Neumann, K.-R. Schulze, K. Unger, *J. Phys. C: Solid State Phys.* **10**, 4709 (1977) https://doi.org/10.1088/0022-3719/10/23/007.
15. Y. Deng, C. Zhang, X. Qin, W. Yan, *Crystals* **15**, 98 (2025) https://doi.org/10.3390/cryst15010098.
16. J.P. Perdew, A. Ruzsinszky, G.I. Csonka, O.A. Vydrov, G.E. Scuseria, L.A. Constantin, X. Zhou, K. Burke, *Phys. Rev. Lett.* **100**, 136406 (2008) https://doi.org/10.1103/PhysRevLett.100.136406.
17. D.R. Hamann, M. Schlüter, C. Chiang, *Phys. Rev. Lett.* **43**, 1494 (1979) https://doi.org/10.1103/PhysRevLett.43.1494.
18. H.J. Monkhorst, J.D. Pack, *Phys. Rev. B* **13**, 5188 (1976) https://doi.org/10.1103/PhysRevB.13.5188.
19. H.A. Ilchuk, I.V. Semkiv, S.I. Krukovskyi, B. Andriyevsky, A.I. Kashuba, *J. Phys. Commun.* (2026) [In Print].
20. A. Kashuba, *Phys. Chem. Solid State* **24**, 92 (2023) https://doi.org/10.15330/pcss.24.1.92-101.
21. W. Nakwaski, *Physica B* **210**, 1 (1995) https://doi.org/10.1016/0921-4526(94)00921-H.
22. J.O. Akinlami, A.O. Ashamu, *J. Semicond.* **34**, 032002 (2013) https://doi.org/10.1088/1674-4926/34/3/032002.

Електронна енергетична структура GaAs легованого Sc

Г.А. Ільчук[1], І.В. Семків[1], С.І. Круковський[1,2], О.С. Кушнір[3], Б. Андрієвський[4], А.І. Кашуба[1]

[1] *Національний університет «Львівська політехніка», 79013 Львів, Україна*
[2] *НДК «Електрон-Карат», 79031 Львів, Україна*
[3] *Львівський національний університет імені Івана Франка, 79017 Львів, Україна*
[4] *Кошалінський технологічний університет, 75453 Кошалін, Польща*

Арсенід галію (GaAs) демонструє широкий спектр практичних застосувань. Зокрема, він широко використовується в оптоелектроніці, де служить основою для високоефективних світлодіодів, лазерних діодів, фотодетекторів та фотоелектричних елементів. Інші важливі застосування включають радіаційно-стійкі сонячні батареї, інтегральні схеми, датчики Холла та інше. У цьому дослідженні повідомляється про концентраційну залежність електронної енергетичної структури для GaAs, легованого Sc ($Ga_{1-x}Sc_xAs$, x = 1/32, 2/32 та 8/32). Розрахунки були виконані в рамках теорії функціоналу густини (DFT) з використанням узагальненого градієнтного наближення (GGA) з параметризацією Пердью–Берка–Ернцергофа (PBEsol). Взаємодію між іонами та валентними електронами було описано за допомогою псевдопотенціалів, що зберігають норму. Досліджено два альтернативні випадки легування Sc в GaAs ($Ga_{1-x}Sc_xAs$, x = 2/32), які відповідають або кубічній (просторова група #215), або тетрагональній (#115) структурам. Проаналізовано дисперсію енергетичних зон та густину станів. Було виявлено, що ширина забороненої зони характеризується прямим переходом при низьких ($x \leq 2/32$) концентраціях Sc, тоді як змінюється на непрямий тип переходу при високих (x = 8/32) рівнях легування Sc. Дисперсію енергетичних зон було проаналізовано на основі розрахованих ефективних мас електронів (m_c) та дірок (m_v). Вплив легування скандієм на електронну енергетичну структуру GaAs було з'ясовано на основі внесків парціальної густини станів (PDOS). Виходячи з електронного енергетичного спектру, ми розрахували дійсну та уявну складові діелектричної функції. Нарешті, фундаментальні оптичні властивості твердих розчинів $Ga_{1-x}Sc_xAs$ отримано за допомогою співвідношень Крамерса-Кроніга, зокрема показник заломлення та коефіцієнти екстинкції та поглинання. На основі електронного енергетичного спектру розраховано дійсну та уявну компоненти діелектричної функції. Нарешті, на підставі співвідношень Крамерса–Кроніга одержано фундаментальні оптичні функції твердих розчинів $Ga_{1-x}Sc_xAs$, зокрема показник заломлення і коефіцієнти екстинкції та поглинання.

Ключові слова: GaAs, Електронна енергетична структура, Густина станів, Заборонена зона, Показник заломлення, Оптична діелектрична функція.